FRACTAL ELLIPTICAL SEGMENT ANTENNA. COMPLETE MATHEMATICAL MODEL AND EXPERIMENTAL APPLICATION

Gheorghe MORARIU*, Ecaterina Liliana MIRON, Tabita DUBEI*, Micsandra ZARA***

*"Transilvania" University, Brasov, Romania,
**"Henri Coanda"Air Force Academy, Brasov, Romania

Abstract: *This paper presents a model for fractal segment antennas with elliptical resonators and resonant slots. Bessel polynomials-based calculation methods were used in order to determine the resonance frequencies. Elliptical contour integration was used for emphasizing the validity of the E-H field transformation phenomenon, according to the Maxwell field dynamics equations. These theoretical fundamental ideas are verified through a series of experiments, rendering charts that are specific to the radiating field intensity, field distribution and the main operational frequency domains. The antenna design was obtained through fractal division based on an isosceles triangle element.*

Keywords: *fractal, antenna, directivity, field intensity, impedance, Bessel functions*

1. INTRODUCTION

Fractal antennas are part of the wideband antenna group, having the widest directivity charts.

This type of antenna has been highly used in mobile communication designs, especially since the beginning of 3G, mainly in stripline models and with median gains over 5dB.

The optimal gain is determined by the reference fractal resonator shape and the number of fractal iterations.

This paper presents a fractal segment antenna model with an elliptical stripline three-level slotted reference resonator.

The resonant frequencies were calculated using the Bessel functions, for the elliptical resonator, and the calculation of frequencies for the slot in a waveguide.

This analytical and practical model yielded positive results in all aspects: frequency domain, directivity chart and emission-reception power, for a median gain of 6 dB.

The analytical considerations for the calculations are the synthesis of papers previously published by our research group, which have resulted in designing and producing the prototype for this antenna.

2. DESIGN PRINCIPLES

The reference stripline resonator has an elliptical shape and is slotted along the major ellipse axis (Morariu, 2013). The resonant frequency calculus is presented (according to (Morariu, 2009) and (Machedon, 2012) as follows:

"*The method consists in the equivalence of common radiating surfaces to those two stripline dipoles superi mposed and separated by the dielectric layer as in Figure 1 neglecting the transfer radiation on the elliptical boundary and dipole plane behind the dielectric (their influence is minimal)*."

This procedure results in a stripline cylindrical resonant cavity, "*whose resonance frequency is derived using the calculation for the variation of high frequency electromagnetic field between plates of the parallel elliptical plane capacitor with dielectric* ε_r" (Machedon, 2012).

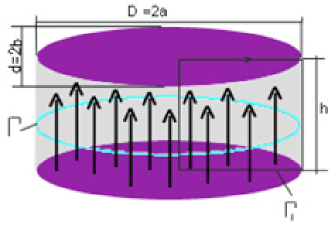

Fig. 1. Stripline equivalent resonator

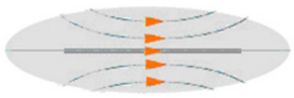

Fig. 2. H_{01} mode

Fig. 3. H_{10} mode

Obtaining the B and E components of the radiating electromagnetic field implies applying the integral form of Maxwell equations iteratively as follows (Machedon, 2012).
The first iteration:

$$S = \pi\, a b \tag{1}$$

$$\hat{\imath} = \frac{\sqrt{a^2 b^2}}{a} \tag{2}$$

where ξ is the eccentricity coefficient.

$$L = 2\pi a P(\xi) \tag{3}$$

$$E\left(\xi, \frac{\pi}{2}\right) = \frac{\pi}{2}\left[1 \neg \left(\frac{1}{2}\right)^2 \xi^2 + \left(\frac{13}{24}\right)^2 \frac{\xi^4}{3} \neg \right.$$
$$\left. \neg \left(\frac{135}{246}\right)^2 \frac{\xi^6}{5} \ldots \right] = \frac{\pi}{2} P(\xi) \tag{4}$$

$$b = a\sqrt{1 \neg \xi^2} \tag{5}$$

$$S = \pi a^2 \sqrt{1 \neg \xi^2} \tag{6}$$

$$\text{Þ} \times E = \frac{\partial}{\partial t} B \tag{7}$$

$$c^2\, \nabla \times B = \frac{\partial}{\partial t} E \tag{8}$$

$$\oint_{\Gamma_2} E\, dl = -\frac{\partial}{\partial t} \int_{\Sigma_{\Gamma_2}} B\, dS \tag{9}$$

$$c^2 \oint_{\Gamma_1} B\, dl = \frac{\partial}{\partial t} \int_{\Sigma_{\Gamma_1}} E\, dS \tag{10}$$

$$E = E_0\, e^{j\grave{u} t} \tag{11}$$

By deriving (10):

$$c^2 B_1 L = \frac{\partial}{\partial t}(E_0\, e^{j\omega t} S) \tag{12}$$

$$c^2 B_1 2\pi a P(\xi) = j\omega E_0 e^{j\omega t} \pi a^2 \sqrt{1 - \xi^2}$$
$$c^2 B_1 2\pi a P(\xi) = j\omega E_0 e^{j\omega t} \pi a^2 \sqrt{1 - \xi^2}$$
$$\tag{13}$$

$$B_1 = \frac{\sqrt{1 - \xi^2}}{P(\xi) 2c^2} a E_0 e^{j\omega t} j\omega \tag{14}$$

By deriving (9):

$$\oint_{\Gamma_2} E\, dl_2 = -E_1\, h = -\frac{\partial}{\partial t} \int_{\Sigma_{\Gamma_2}} B_1\, dS_2 \tag{15}$$

For $dS_2 = h\, da$:

$$E_1 h = \frac{\partial}{\partial t}\left(j\omega \int_0^a \frac{\sqrt{1 - \xi^2}}{P(\xi) 2c^2} E_0 e^{j\omega t} a h da \right)$$
$$E_1 h = \frac{\partial}{\partial t}\left(j\omega \int_0^a \frac{\sqrt{1 - \xi^2}}{P(\xi) 2c^2} E_0 e^{j\omega t} a h da \right) \tag{16}$$

$$E_1 == -\frac{\sqrt{1 - \xi^2}}{P(\xi)} E_0 e^{j\omega t} \frac{\omega^2 a^2}{4c^2} \tag{17}$$

After three iterations of derivation (minimum) and taking into consideration that

$$\overline{E} = \overline{E}_0 + \overline{E}_1 + \overline{E}_2 + \overline{E}_3 + \ldots \tag{18}$$

$$\frac{\omega b}{2c} = \frac{x}{2}, \tag{19}$$

the final relation is:

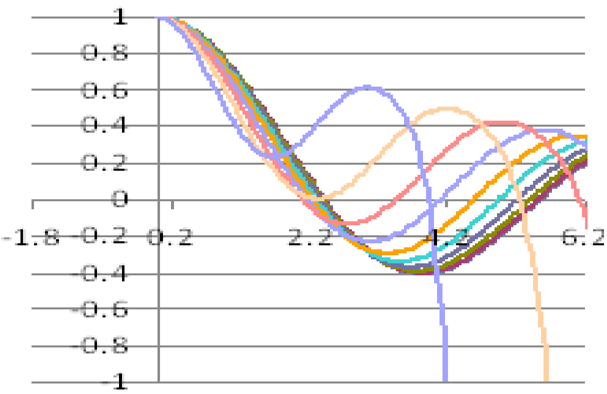

Fig. 4. H(x,ξ) chart as for the major ellipse axis

$$\bar{E} = E_0 e^{j\omega t}\left(1 - \frac{1}{P(\xi)} + \frac{1}{P(\xi)}\left(1 - \frac{1}{(1!)^2}\left(\frac{x}{2}\right)^2 \frac{1}{\sqrt{1-\xi^2}} + \frac{1}{(2!)^2}\left(\frac{x}{2}\right)^4 \frac{1}{\left(\sqrt{1-\xi^2}\right)^3} - \dots\right)\right)$$

(20)

$\bar{E} = E_0 e^{j\omega t} \cdot H(x, \xi)\bar{E} = E_0 e^{j\omega t} \cdot H(x, \xi)$

(21)

$H(x,0) = J_{01}(x)H(x,0) = J_{01}(x)$ it is a Bessel function which can be applied for elliptical resonant surfaces (Morariu, 2009).

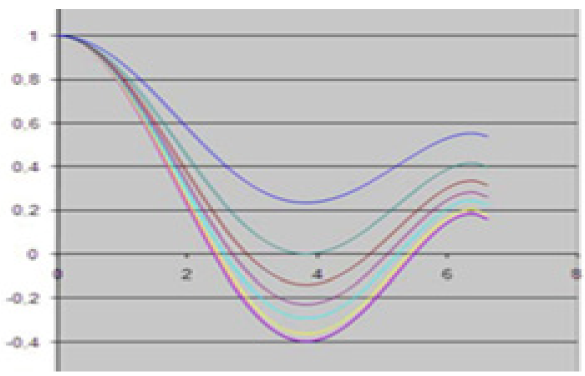

Fig. 5. H(x,ξ) chart for the minor axis of the ellipse

A planar resonant cavity is positioned symmetrically on every major axis of the ellipses, with the following parameters.

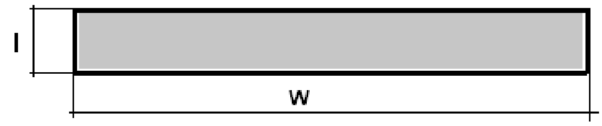

Fig. 6. Stripline resonant cavity [11]

The dynamics of the electric field derives from the electromagnetic wave equation of the plane resonant cavity.

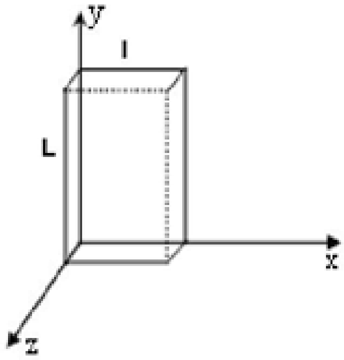

Fig. 7. Model of the plane resonant cavity

The electromagnetic wave equation of the plane resonant cavity is:

$$\frac{\partial^2 H_z}{\partial x^2} + \frac{\partial^2 H_z}{\partial y^2} + \mu\varepsilon\omega^2 H_z = 0 \qquad (22)$$

Considering the following conditions:
$E_z = 0$, $x = 0$ and $x = l$;
$E_z = 0$, $y = 0$ and $y = L$,
the value for H_z can be calculated:

$$H_z = H_0 \cos\left(n\pi\frac{x}{l}\right)\cos\left(m\pi\frac{y}{L}\right)$$

$$H_z = H_0 \cos\left(n\pi\frac{x}{l}\right)\cos\left(m\pi\frac{y}{L}\right) \qquad (23)$$

for $0 \le x \le l$ and $0 \le y \le L$.

Specific resonance pulsation for the propagation mode:

$$\omega = \frac{\pi}{\sqrt{\varepsilon\mu}}\sqrt{\frac{n^2}{l^2} + \frac{m^2}{L^2}} \qquad (24)$$

$$\lambda_{rez} = \frac{2\sqrt{\varepsilon_r}}{\sqrt{\frac{n^2}{l^2} + \frac{m^2}{L^2}}} \quad (25), \qquad L = \frac{\lambda_r}{2} \quad (26)$$

The H_{01} propagation mode is dominant, rendering n=0 and m=1.

$$\omega_r = \frac{4\pi \cdot c}{\lambda_r \sqrt{\varepsilon_r}} \pi r^2 \, , \; f_r = \frac{2c}{\lambda_r \sqrt{\varepsilon_r}} \qquad (27)$$

where $\varepsilon_r \cong 2{,}25$.

Table 1. Slot resonator frequencies for the three fractal iterations, Propagation mode H_{01}

Slot length [m]	Frequency [GHz]
0.032	4.1667
0.048	2.778
0.059	2.259

Considering x = ωb/c and y = ωa/c, the resonant frequencies and corresponding harmonics can be identified.

Table 2. Elliptical resonator frequencies for the minor axis of the ellipse [GHz]

	b1	b2	b3
Length[m]	0.035	0.025	0.017
2.1	2.87	4.01	5.90
2.1 x2	5.73	8.03	11.80
2.3	3.14	4.39	6.46
2.3 x2	6.28	8.79	12.93
3.45	4.71	6.59	9.69
3.45 x2	9.42	13.18	19.39
3.95	5.39	7.55	11.10
3.95 x2	10.78	15.10	22.20
5.25	7.17	10.03	14.75
5.25 x2	17.33	20.06	29.51

Table 3. Elliptical resonator frequencies for the major axis of the ellipse [GHz]

	a1	a2	a3
Length [m]	0.087	0.066	0.05
2.1	1.15	1.52	2.01
2.1x2	2.31	3.04	4.01
2.3	1.26	1.66	2.20
2.3x2	2.53	3.33	4.39
3.45	1.89	2.50	3.30
3.45x2	3.79	4.99	6.59
3.95	2.17	2.86	3.77
3.95x2	4.34	5.72	7.55
5.25	2.88	3.80	5.02
5.25x2	5.77	7.60	10.03

Table 4. Variable elliptical waveguide behavior

a [m]	Dipole frequency [GHz]
0.051	0.980
0.069	0.724
0.091	0.549
0.1255	0.398
0.1765	0.283
0.1	0.5

Table 5. Linear equivalent dipole behavior

λ/4 [m]	Frequency [GHz]
0.09	0.857
0.105	0.480
0.155	0.375

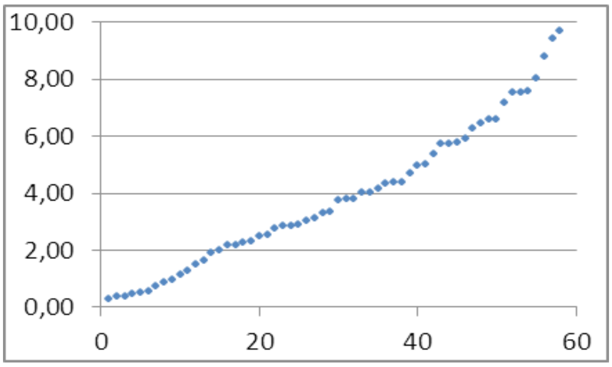

Fig. 8. Experimental frequency spectrum distribution

3. EXPERIMENTAL APPLICATION

According to the previous mathematical description, an experimental model of an antenna with fractal elliptical segments was designed (Morariu, 2013). The antenna has the following parameters.

A. Antenna Architecture

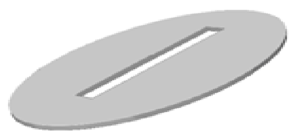

Fig. 9. The main resonator shape (Machedon, 2012)

The fractal generation was based on the isosceles triangle division, with a triangle side ratio equal with the axis ratio of the ellipse:

$$\frac{D_n}{d_n} = \frac{k \cdot L_n}{\frac{B_n}{2}}$$

where k is the surface constant.
The ratio $base_{n+1} = l_n/2$, is maintained.

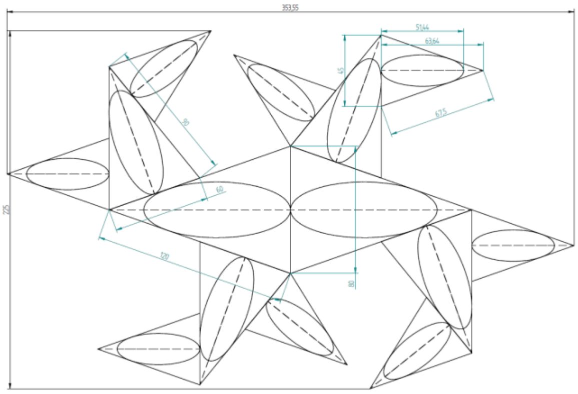

Fig. 10. Antenna design – triangle fractal division

Initial dimensions: k = 0.9; d_0 = 3.8cm; D_0 = 9.14cm; L_0 = 12cm.

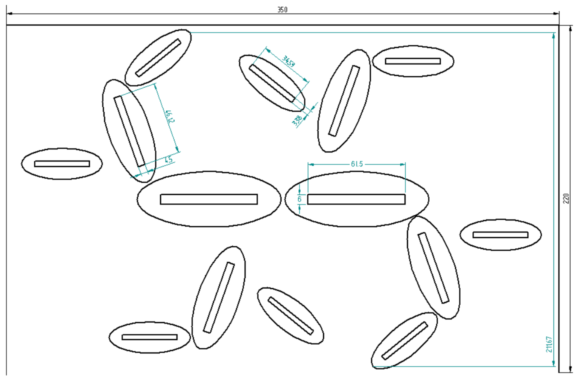

Fig. 11. Fractal antenna with elliptical dipoles – front side

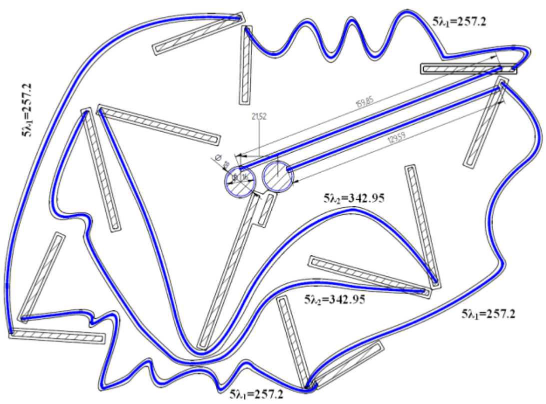

Fig. 12. Fractal antenna with elliptical dipoles back view (full line–phase connection; hatched line–feeder matching segments)

B. Experimental Results

The experimental analysis for the antenna was conducted for two frequency domains: below 1GHz (using scalar spectrum analyzer) and from 1GHz to 18GHz using a VNA (vector network analyzer). The main results are presented in the following section (Morariu, 2013).

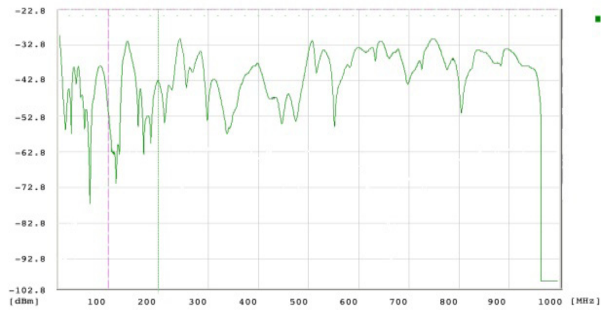

Fig. 13. Frequency spectral diagram – reception

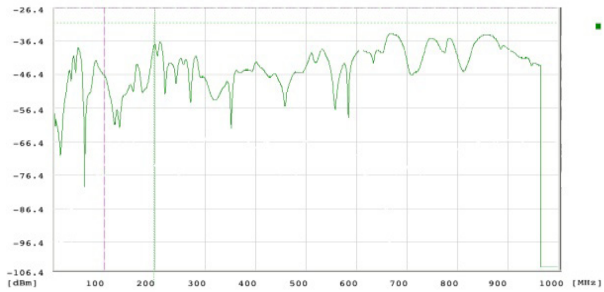

Fig. 14. Frequency spectral diagram - emission

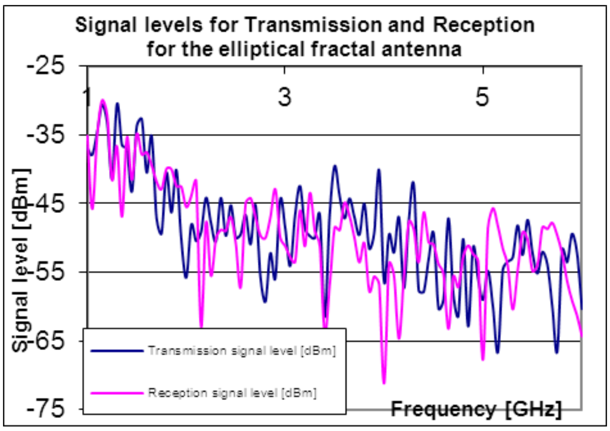

Fig. 15. Signal levels E/R for 1-6GHz

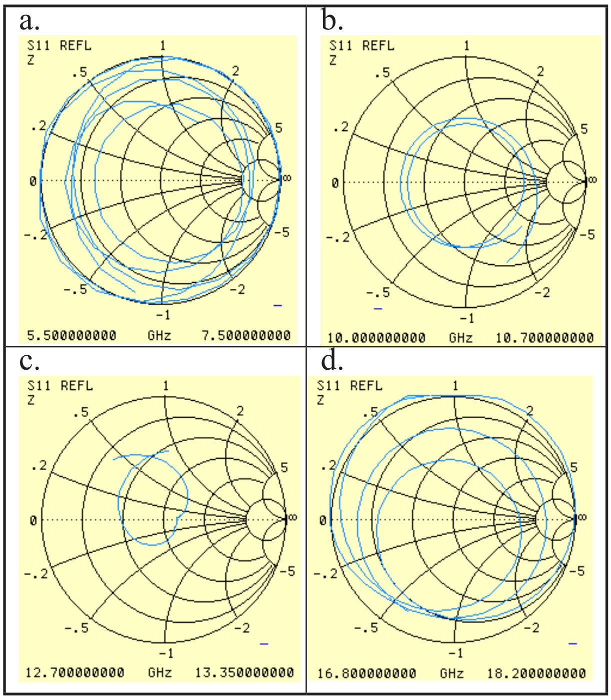

Fig. 16. Smith charts obtained for the frequency domains:
a. 5.5-7.5GHz; b. 10-10.7GHz;
c. 12.7-13.35GHz; d. 16.8-18.2GHz

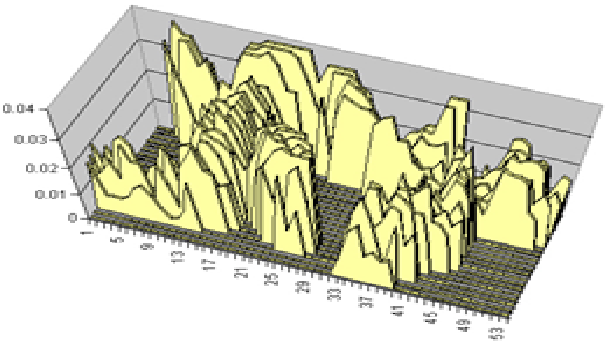

Fig. 17. E field distribution for the radiant elements

The fractal antenna with elliptical segments has a wide directivity chart (fig. 18)

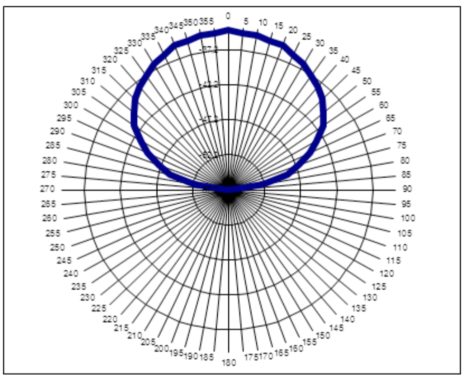

Fig. 18. Directivity chart for the E parameters

CONCLUSIONS

The following aspects can be noted regarding the design and prototyping of the fractal segment antenna with elliptical dipoles:

The analytical calculations and the experimental results yield the same conclusions for 98 percent of the considered aspects, which confirms the theoretical hypothesis.

The frequency domains that were obtained through experiments are even larger than the theoretical estimations, this being a result of the interference between the fractal elements.

The minimum gain for marginal frequencies is larger than 5 dB.

The directivity diagram is wide (approx. 160°) and makes the antenna suitable for mobile communication handheld devices (for small dimensions) as well as base stations, for larger dimensions, given that the emission-reception power is sufficient for an optimal coverage.

BIBLIOGRAPHY

1. Amman, M. (1997). Design of Rectangular Microstrip Patch Antennas for the 2.4 GHz Band. Applied Microwave&Wireless, pp. 24-34.
2. Evangelos, S.A., et.al. (2006). Circular and Elliptical CPW-Fed Slot and Microstrip-Fed Antennas for Ultra wideband Applications. IEEE Antennas and Wireless Propagation Letters, vol. 5, pp. 294-297.
3. Liang, G., Liu, Y., Mei, K.K. (1989). Full-wave analysis of coplanar waveguide and slotline using the time domain finite-difference method. IEEE Transactions on Microwave Theory and Techniques, vol. 17, pp. 1949-1957.
4. Machedon-Pisu, M., Morariu, G. (2012). New Calculation Methods for Stripline Resonators of Elliptic type and Application. Proceedings Of The 13Th International Conference On Optimization Of Electrical And Electronic Equipment, ISSN 1842-0133, pp. 1193-1198.
5. Marchais, C., Le Ray, G., Sharaiha, A. (2006). Stripline slot antenna for UWB communication. IEEE Antennas and Wireless Propagation Letters, vol. 5, pp. 319-322.
6. Morariu, Ghe., Alexandru, M., Miron, M., Romanca, M., Machedon-Pisu, M., Dobrescu, A. (2009). Experiment-supported study on the bipolar disk microstrip antenna. EU Annals of DAAAM & Proceedings, Vienna, Austria. ISSN 1726-9679/ISBN 978-3-901509-70-4.
7. Morariu, G., Zara, M. (2013) Fundamente si aplicatii ale structurilor fractale in antene pentru microunde. Editura Universitatii Transilvania din Brasov. ISBN 978-606-19-0270-5.